Analysis of Chips Geometry and Parametric Optimization using Grey Relational Analysis (GRA) in Hot Turning of AISI 202

Subhas Chandra Moi[1], Rajeev Ranjan[2]*

[1,2]Department of Mechanical Engineering, Dr. B. C. Roy Engineering College, Durgapur- 713206, Bharat

*Author to whom correspondence should be addressed:
E-mail:rajeevranjan.br@gmail.com

(Received December 12, 2023; Revised February 23, 2024; Accepted February 29, 2024).

Abstract: Hot turning is a method that assists in metal cutting by applying heat, especially useful for dealing with difficult-to-machine materials. Such challenging materials typically possess unique characteristics, including exceptional strength at high temperatures (referred to as hot strength), low ability to conduct heat, and a tendency to become harder during machining. As a result, machining these materials leads to increased cutting forces, higher specific power consumption, quicker tool wear, and compromised quality of the machined surface. To improve machining efficiency, one can utilize the concept of hot machining, which involves using an external heat source to heat the workpiece before machining. This preheated workpiece becomes softer, improving tool life, surface finish, and power consumption while facilitating the removal of material with less cutting effort and tool wear. To improve surface quality and the material removal rate (MRR), which is always desirable for any machining operation, AISI 202 steel which is widely used in the automotive, aerospace, and electrical machinery industries was subjected to a hot turning process in this research study. The effort focused on maximizing material removal rate and lowering surface roughness utilizing the GRA approach to assess the optimal process environment that may concurrently satisfy both quality and productivity objectives. Special focus was also given to chip geometry. The results indicate that temperature has the greatest influence on not only equivalent chip thickness but also surface roughness and MRR, followed by cutting speed and cutting depth.

Keywords: hot turning; chip geometry; GRA; surface roughness; MRR; AISI 202

1. Introduction

High-strength materials are essential to many sectors, including aerospace, space exploration, nuclear engineering, biomedical technology, and the automotive sector. However, machining these materials is a challenging task that often requires expensive cutting tools[1-4]. To address this challenge, hot machining is employed, a method that utilizes heat to soften the workpiece, minimizing its shear strength and making it easier to cut. This thermal softening results in lower cutting forces, leading to reduced tool wear[5]. Hot machining offers several advantages over conventional machining techniques, including improved surface quality, reduced chip formation, prolonged tool life, and lower power consumption. Previous research has investigated the performance of hot machining on hardened alloys, superalloys, and ceramic materials, using various heat sources like lasers, plasma arcs, acetylene gas, and induction coils[6]. These studies consistently confirm the effectiveness of hot machining in reducing cutting forces and enhancing surface quality. Nickel and its alloys, due to their low thermal conductivity, low elasticity modulus, and reactivity with cutting tools at high temperatures, pose challenges during machining. These results in elevated temperatures, pressure, and stress at the cutting edge, leading to rapid tool wear and increased machining forces[7]. Hot machining effectively addresses these challenges without compromising productivity or quality. By heating the workpiece to its recrystallization temperature, hot machining reduces forces, minimizes tool wear, and extends tool life[8-10]. Numerous researchers have explored heat-assisted machining of nickel-based materials using various heating sources, consistently observing benefits such as improved surface finish, reduced cutting forces, and decreased tool wear[11-15]. One common issue during machining is chip segmentation, which directly impacts cutting forces and machinability[16]. Cryogenic machining is a method that reduces adhesion between the workpiece and cutting tool, minimizing the formation of built-up edges and lowering the chip-tool friction coefficient[17]. This approach also addresses the formation of chatter and tool/spindle vibrations associated with serrated chip formation, which affects both turning

and milling operations[18]. Additionally, plastic properties and thermal conductivity play roles in chip segmentation[19-20]. Qibiao et al. researched to analyze the distinctive features of both continuous and serrated chip formation. They elucidated continuous chip formation by examining factors such as chip deformation, strain, and strain rate. On the other hand, they associated serrated chips with the extent of segmentation and the frequency of serration[21]. Schulze et al. explored the effect of cutting speed and feed per tooth on the degree of segmentation in aluminum machining, noting an increase[22]. Researchers have also delved into the mechanism behind serrated chip formation in plastic materials, referring to it as catastrophic thermoplastic shear instability. Hua and Shivpuri[23] emphasized the significant roles that chip morphology and segmentation play in determining tool wear and material machinability. Excessive vibration during chip segmentation can negatively affect productivity and material removal rates. errated chips are believed to develop when the softening influence in the primary region surpasses the strain-hardening impact. Gao et al.[24] conducted a review of chip segmentation in titanium alloy machining. In hot machining processes, understanding chip formation, particularly segmentation and cyclic cutting forces, is challenging due to complex thermo-mechanical phenomena. Typically, segmentation occurs within an adiabatic shear band, resulting in thermal softening rather than strain hardening. Experimentally modeling the chip formation process is a time-consuming and expensive endeavor. Interestingly, under certain ductile or alternative cutting conditions, segmentation can occur without damaging the chip[25]. Lin and Lin[26] conducted research on crack initiation and propagation within the chip, using finite element analysis to validate their experimental results. The primary cause of initiating adiabatic shear bands and transforming continuous chips into serrated ones during the machining of hardened steel is thermo-mechanical instability in the primary zone[27]. Bouchank and colleagues[28] found that when thermal assistance is used in machining processes, it brings about changes in the sawtooth patterns, causing a reduction in sawtooth heights as opposed to what is observed in conventional machining. Conversely, in cryogenic machining settings, there is an increase in the frequency of chip serration, along with a decrease in the average shear band thickness. Notably, there has been limited attention given to examining the influence of heating methods like laser heating on chip geometry or morphology, and there has been no investigation into chip characteristics using numerical modeling. Parida[29] conducted a study to examine the influence of heating temperature on the forces exerted and the geometry of chips. Additionally, they utilized numerical analysis to assess various parameters, including chip thickness, length of the shear plane, degree of segmentation, and other related factors. Their findings were compared to previous research[30], showing good agreement. Hanief et al.[31] introduced artificial intelligence techniques, specifically the genetic algorithm (GA), to optimize parameters during the hot turning of Monel-400. A novel approach proposed by Airao et al.[32] combines pre-heating and ultrasonic vibration to analyze responses during the cutting of difficult-to-cut materials. Response surface methodology (RSM) was used to construct mathematical models to predict surface roughness in hot machining of an AISI 4340 in lathe[33-34].

From the literature review, it is evident that there has been limited research on analyzing chip characteristics in hot machining. The present study focuses on the impact of heating temperature on chip geometry and surface texture. Additionally, to optimize process parameters, such as material removal rate and surface roughness we applied grey relational analysis (GRA).

2. Experiment Procedures

The center lathe was utilized for all cutting experiments. During the heating process, the workpiece was rotated slowly to ensure uniform heating. An Oxyacetylene gas flame was employed to heat the workpiece. To monitor the work surface's temperature, a thermocouple was connected to a temperature display system. The flame control mechanism was connected to an automated controller. The workpiece was heated until it reached the specified temperature after first setting the desired heating temperature on the temperature display device. Once the desired temperature was achieved, the flame control mechanism would autonomously retreat from the workpiece and return whenever the temperature decreased. Table 1 provides the chemical compositions of AISI 202. The carbide cutting tool had the following properties: a density of 11,900kg/m^3, Young's modulus of 63GPa, Poisson's ratio of 0.26, yield strength of 4250MPa, thermal expansion coefficient of 5.4 x 10^{-6}, specific heat of 334J/kgK, and thermal conductivity of 100Wm^{-1}K^{-1}. Figure 1 illustrates the heating system along with the schematic diagram of orthogonal machining. A cylindrical rod with an outer diameter of 50mm was used as the workpiece material.

Table 1. Chemical components of AISI 202

Chemical analysis							
C	**Mn**	**Si**	**S**	**P**	**Cr**	**Ni**	**Fe**
0.07%	10.80%	0.48%	0.02%	0.02%	15.10%	0.39%	73.01

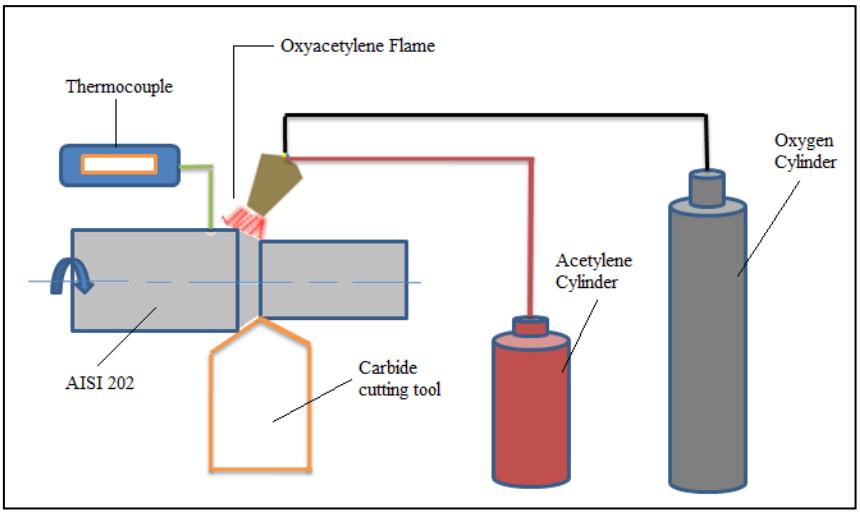

Fig.1: Experimental arrangement

2.1 Grey Relational Analysis (GRA)

GRA is a method used to identify the most favorable settings for multiple input factors to attain the highest quality characteristics[35-36]. It relies on the principles of Grey system theory, which can effectively address a variety of performance metrics. Optimizing complicated outputs can thus be reduced to optimizing a single grey relational grade (GRG). GRA is used to identify whether or not there is consistency between two factors shifting patterns, as well as the most likely mathematical relationship between the factors or within the components themselves.

2.1.1 Data pre-processing

Data pre-processing is typically essential as data sequences may exhibit variations in their range and units. When there's considerable variability in the spread of values across sequences or differences in the target directions they represent, data pre-processing becomes a requisite step[37-38]. The process of transforming an initial sequence into a standardized one is commonly referred to as data pre-processing. Various techniques for data pre-processing in the context of grey relational analysis are available, depending on the specific characteristics of the data sequence. In cases where the original sequence has an infinite target value, it is designated as having a "higher is better" condition. To address this, the original sequence has been subjected to normalization as follows:

$$x_i^*(k) = \frac{x_i^o(k) - min\, x_i^o(k)}{\max x_i^o(k) - \min x_i^o(k)} \quad (1)$$

When the original sequence has the "lower is better" attribute, the original sequence should be normalized as follows:

$$x_i^*(k) = \frac{\max x_i^o - x_i^o(k)}{\max x_i^o(k) - \min x_i^o(k)} \quad (2)$$

2.1.2 Grey relational coefficient and grey relational grade (GRG)

In the context of grey relational analysis, the grey relational grade (GRG) serves as an indicator of the connection or relevance between two systems or sequences. When we have a single reference sequence, denoted as $x^o(k)$, and several other sequences used for comparison, we engage in a specific form of analysis known as local grey relation measurement. After preparing and organizing the data, we can express the grey relation coefficient $i(k)$ for the kth performance characteristic of the ith experiment as follows:

$$\xi(k) = \frac{\Delta_{min} + \xi.\Delta_{max}}{\Delta_{oi}(k) + \xi.\Delta_{max}} \quad (3)$$

In the given context, $\Delta_{oi}(k) = |x_o^*(k) - x_i^*(k)|$ represents the absolute difference between the reference sequence $x_o^*(k)$ and the comparability sequence $x_i^*(k)$. The parameters Δ_{max} and Δ_{min} are set at 1.00 and 0.00, respectively, while $\Delta_{oi}(k)$ denotes the deviation sequence. The coefficient ξ termed the distinguishing or identification coefficient, is defined within the range $0 \leq \xi \leq 1$, with the option to adjust its value based on practical system requirements. A smaller ξ value corresponds to greater distinguishing ability.

The purpose behind introducing this coefficient is to quantify the relational degree between the reference sequence $x_o^*(k)$ *and the comparability sequence* $x_i^*(k)$, with ξ typically set at 0.5. Subsequently, after obtaining the grey relational coefficient, it is customary to compute the average of these coefficients to determine the GRG. The GRG is outlined as follows:

$$\gamma_i = \frac{1}{n}\sum_{k=1}^{n} \xi_i(k) \quad (4)$$

However, the relative relevance of these components fluctuates in an actual engineering system. The GRG in Eq. 1 was extended and defined as advised by Deng (1982) under the genuine circumstance of unequal weight

carried by the various components.

$$\gamma_i = \frac{1}{n}\sum_{k=1}^{n} w_k \xi_i(k) \quad (5)$$

Where $\sum_{k=1}^{n} w_k = 1$ is used to indicate that the sum of normalized weights for various factors equals *k*. The term w_k refers to the weight assigned to each factor after normalization. The γi, known as the grey relational grade (GRG), represents the level of correlation between the reference sequence and the comparison sequence. If the two sequences are identical, the GRG reaches a value of 1.

Moreover, the GRG provides a perspective on the degree of impact exerted by the comparison sequence on the reference sequence. Therefore, when a particular comparison sequence holds greater importance for the reference sequence in comparison to others, the GRG between that specific comparison sequence and the reference sequence will exceed that of the others. Grey relational analysis entails evaluating the absolute data disparity between sequences and can be utilized to estimate an approximate correlation.

3. Result and discussion

3.1 Impact of Temperature Variations on Chip Morphology

The research examined chip thickness under various heating temperatures, measured at different positions, and then calculated the average. The findings revealed that as the heating temperature increased, the chip thickness decreased. Figure 2 illustrates the relationship between chip thickness and heating temperature.

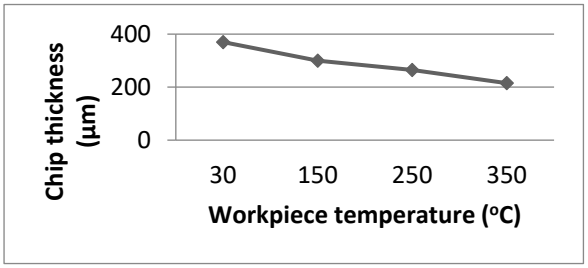

Fig.2: Workpiece temperature vs chip thickness

The chip formation process in machining is influenced by three distinct zones. These areas consist of the primary zone, which is associated with shearing; the secondary zone, identified by the friction between the tool and the chip; and the tertiary zone, where friction arises between the work surface and the tool's flank face. The temperature generated during hot machining has a considerable impact on the primary shear zone, resulting in changes in chip characteristics, chip shape, cutting forces, residual stresses, and various related factors[28-30].

It was noted that when machining was conducted at ambient temperature, the chip thickness was greater in comparison to machining carried out at elevated temperatures. Figure 3 illustrates the chip morphology achieved when machining AISI 202 with an uncoated carbide tool under room temperature and high-temperature conditions. Two distinct chip types were observed during the AISI 202 machining process. Turning at room temperature resulted in short and sporadic chips, while higher temperatures led to the formation of continuous chips. The majority of the chips produced at both room and elevated temperatures exhibited a helical shape.

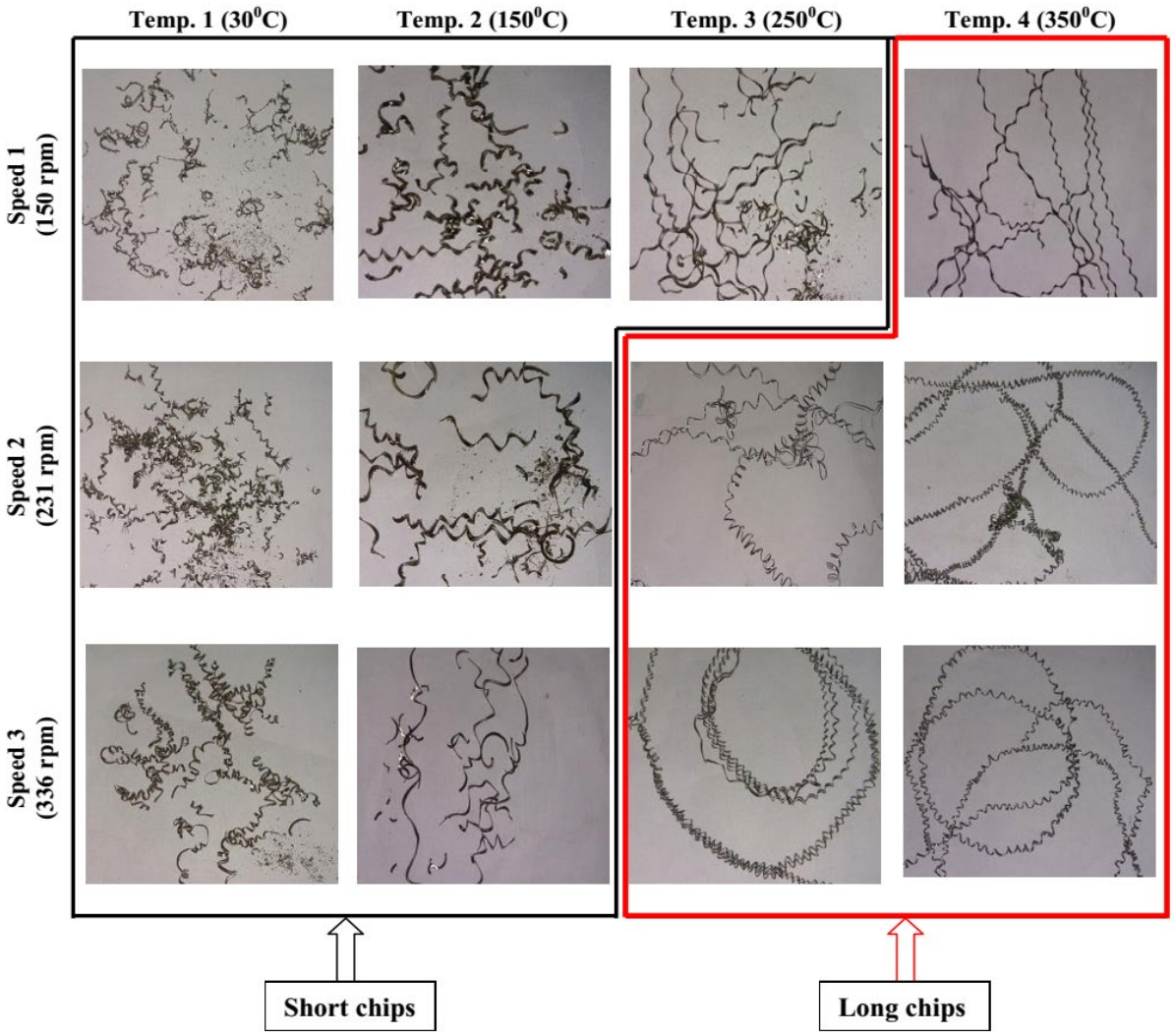

Fig.3: Chip formation in different heating conditions

Figure 3 illustrates the absence of chips on the surfaces resulting from various cutting speeds. At a relatively low cutting speed of 150 rpm, a regular-shaped ductile chip tearing phenomenon was observed within the inner circle of the chip, specifically in the corner section formed near the tool's nose edge. Nevertheless, when the cutting speed was elevated to 231 and 336 rpm, there was observed irregular tearing of the ductile chip along the outer circumference. This variation can be associated with the way the chip material reacts, showing increased resistance to deformation at lower cutting speeds and becoming more pliable at higher cutting speeds. When the cutting speeds were lower, the workpiece material displayed a brittle nature, displaying little susceptibility to alterations in strain rate or temperature. Conversely, higher cutting speeds resulted in increased material ductility and elevated cutting temperatures[39].

3.2 Parametric optimization using GRA

Grey Relational Analysis (GRA) is a quantitative method for examining how several parameters relate to one another within a system[40-41]. A collection of observations is used to compare the behavior of several components to determine how correlated they are. This is accomplished by figuring out the gray relational coefficient, which shows how closely each factor is correlated. Following the processes outlined above, grey relational analysis was performed using experimental data to reduce the large number of replies to a single objective problem. In the current work, MRR must be maximised to improve material removal, while surface roughness (Ra) must be minimised to get a superior surface texture. The experimental data for MRR and surface roughness (Ra) were normalised using Eqs. (1) and (2), which are provided in Table 2 as grey relational generations. The grey relational coefficient was computed using the pre-processing data shown in Table 2. Table 3 shows the Δ_{0i} values and Grey relational values, as well as their grades and ordering.

Table 2. RSM design matrix, input, output responses and Grey Relational generation values

						Ra	MRR
Ideal Sequence	Speed (RPM)	DOC (mm)	Temperature (^{0}C)	Surface Roughness, Ra (µm)	MMR (cm3/min)	Smaller-the-better	Greater-the-better
1	150	0.25	250	1.915	0.336	1.915	0.336
2	336	0.25	250	0.969	0.306	0.969	0.306
3	150	0.75	250	0.613	0.354	0.613	0.354
4	336	0.75	250	0.891	0.952	0.891	0.952
5	150	0.5	150	2.912	0.359	2.912	0.359
6	336	0.5	150	2.254	0.673	2.254	0.673
7	150	0.5	350	0.658	0.179	0.658	0.179
8	336	0.5	350	0.695	0.442	0.695	0.442
9	243	0.25	150	4.835	0.341	4.835	0.341
10	243	0.75	150	1.713	0.7	1.713	0.7
11	243	0.25	350	0.619	0.16	0.619	0.16
12	243	0.75	350	2.462	0.459	2.462	0.459
13	243	0.5	250	1.338	0.393	1.338	0.393
14	243	0.5	250	1.245	0.391	1.245	0.391
15	243	0.5	250	1.246	0.392	1.246	0.392

Table 3. Grey relationship coefficient and its grade values

Sl. No	Assessment of Δ_{Oi}		Grey relationship coefficient		GRG	Rank
	Ra	MRR	Ra	MRR		
Ideal Sequence	1	1	1	1		
1	0.692	0.222	0.591	0.818	0.705	5
2	0.916	0.184	0.522	0.844	0.683	6
3	1.000	0.245	0.500	0.803	0.652	11
4	0.934	1.000	0.517	0.500	0.509	15
5	0.455	0.251	0.687	0.799	0.743	3
6	0.611	0.648	0.621	0.607	0.614	13
7	0.989	0.024	0.503	0.977	0.740	4
8	0.981	0.356	0.505	0.737	0.621	12
9	0.999	0.000	0.500	1.000	0.750	2
10	0.739	0.682	0.575	0.595	0.585	14
11	0.000	0.229	1.000	0.814	0.907	1
12	0.562	0.378	0.640	0.726	0.683	7
13	0.828	0.294	0.547	0.773	0.660	8
14	0.850	0.292	0.540	0.774	0.657	9
15	0.850	0.293	0.541	0.773	0.657	10

3.2.1 Developing the mathematical model GRG

In the current study, regression analysis was used. The trial data was run through Design-Expert 11 software to generate quadratic mathematical equations for Grey Relational Grade (GRG). This set of regression equations/mathematical model is used to predict responses (GRG) in terms of speed (A), depth of cut (B), and temperature (C). It is made up of the effect of the primary parameters as well as the first-order interaction of all parameters. The ANOVA (analysis of variance) is used to investigate GRG and identify the impact of each parameter on multi-objective optimization. The ANOVA analysis for single objective optimization is shown using Design-Expert 11 statistical software.

3.2.2 Grey Relational Grade (GRG)

The following coded factors are used to build the response to the second-order regression equation for surface roughness:

$$GRG = 1.31653 + 0.002065*A - 0.877339*B - 0.004297*C - 0.001301*A*B + 2.68817E - 07*A* C + 0.002550*B*C - 4.19124E - 06*A^2 + 0.248000*B^2 + 5.77500E - 06*C^2$$

Table 4 shows the proper ANOVA test results for surface roughness (GRG), and the model is found to be significant (P0.05) at 95% confidence or 5% significant level. The model's lack of fit value is minor, which is good. Its F-value is 12.95, indicating that it is significant. The model shows that the hot turning process parameters speed (A), depth of cut (B), temperature (C), and its squared terms [speed (A^2), depth of cut (B^2), temperature (C^2)] and interaction effects [speed depth of cut (A * B), speed temperature (A * C), depth of cut temperature (B * C)] have a major impact on surface roughness. The R^2 value is 0.9589, while the Pred R^2 is 0.3427, which accords with the Adj R^2 value of 0.8848. The value of R^2 is greater and closer to one, which is better.

Table 4. ANOVA results for Grey Relational Grade (GRG)

Sources	S.S	D.F	M.S	F-Value	P-Value	
Model	0.1083	9.0	0.0120	12.95	0.0058	Significant
A : Speed	0.0213	1.0	0.0213	22.96	0.0049	Significant
B : Depth of cut	0.0004	1.0	0.0004	0.4071	0.4515	Significant
C : Temperature	0.0474	1.0	0.0474	51.07	0.0008	Significant
A*B	0.0037	1.0	0.0037	3.94	0.1039	not significant
A*C	0.0000	1.0	0.0000	0.0269	0.8761	not significant
B*C	0.0163	1.0	0.0163	17.50	0.0086	not significant
A*A	0.0049	1.0	0.0049	5.22	0.0710	not significant
B*B	0.0009	1.0	0.0009	0.9551	0.3733	not significant
C*C	0.0123	1.0	0.0123	13.26	0.0149	not significant
Residuals	0.0046	5.0	0.0009			
Lack of Fits	0.0046	3.0	0.0015	515.31	0.0019	not significant
Error	6.000E-06	2.0	3.000E-06			
Total	0.1129	14.0				

$R^2 = 0.9589$, Adjusted $R^2 = 0.8848$, Predicted $R^2 = 0.3427$, Adeq Precision = 16.0953

3.2.3 Model validation GRG

Figure 4 compares anticipated and actual values of the response variable GRG. The graphs illustrate that the provided models are adequate. It also means that the expected results are consistent with the measured data.

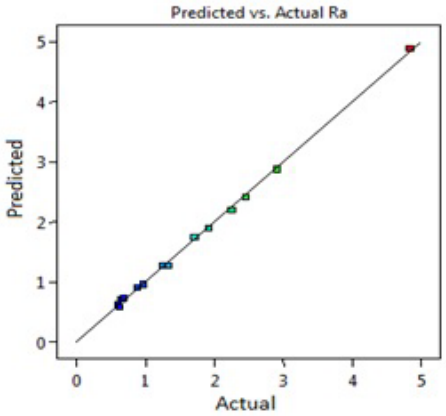

Fig.4: Predicted vs actual plot of (C) GRG

3.2.4 The effect of process factors on GRG

Figure 5 and Figure 6 depict the response surface plot and contour plot, which are used to explore the interaction effects of input process parameters on GRG. GRG has similar patterns. GRG consistently increases with increasing hot-turning input parameters up to a threshold value and then begins to diminish. GRG performs best at medium hot turning speed, temperature, and cut-depth values. The temperature has the biggest influence on GRG, followed by hot turning cutting speed, and cut depth.

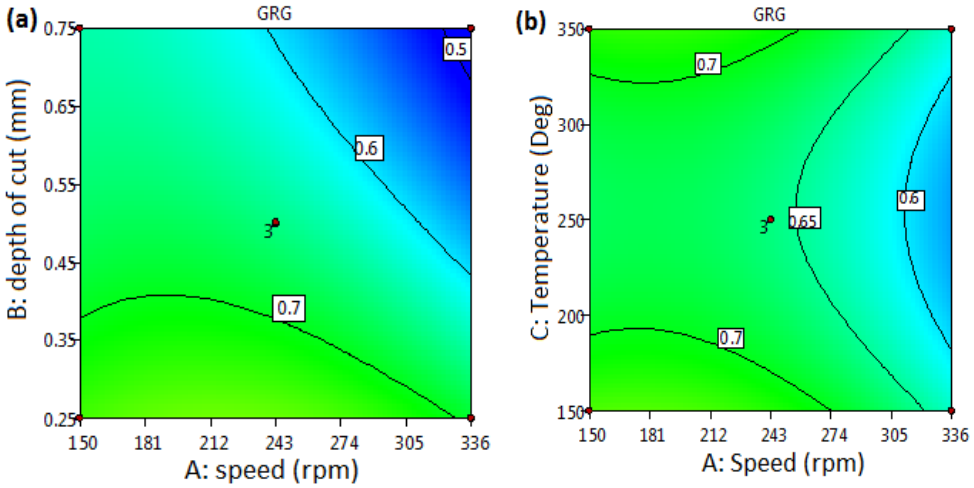

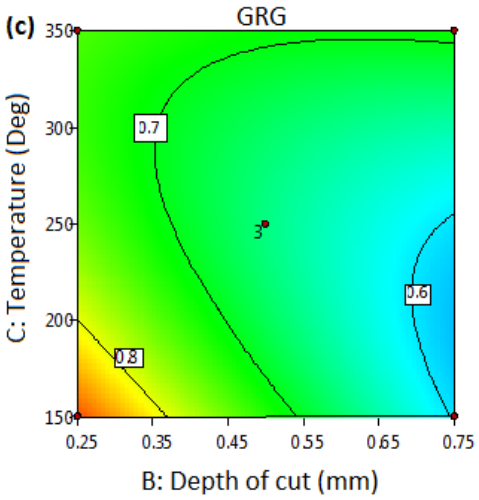

Fig.5: Contour graphs depicting the interactions of (a) speed vs depth of cut, (b) speed vs temperature and (c) depth of cut vs temperature on GRG

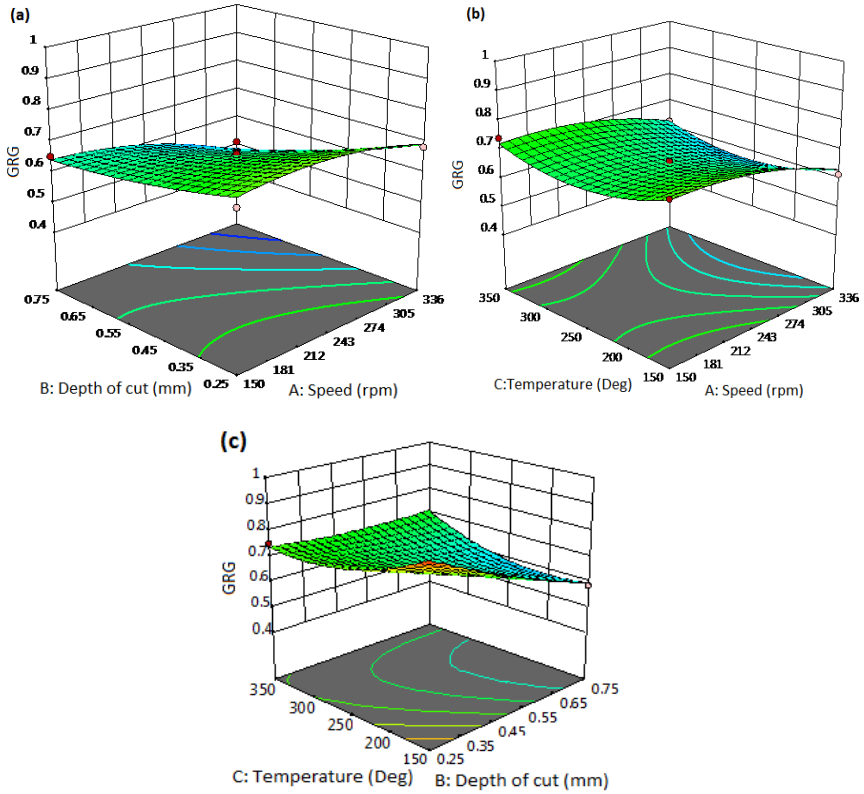

Fig.6: Plots of the response surface illustrating the interaction effects of (a) speed vs depth of cut, (b) speed vs temperature, and (c) depth of cut vs temperature on GRG

3.2.5 Numerical Optimization (GRG)

Figure 5 and Figure 6 show the graphs (response surface plot and contour plot) used to investigate the intermediate effects of input process factors on GRG. GRG has similar types of patterns. GRG steadily grows with increasing hot-turning input process factors up to a certain limit and then begins to decrease. GRG is most effective at medium hot turning speed, temperature, and depth of cut parameters. Temperature is the most important aspect of GRG, followed by hot turning speed (cutting) and depth of cut. The desired function technique was used in the optimization procedure to optimize the material removal rate (MRR) while retaining minimal surface roughness. Figure 7 depicts the results.

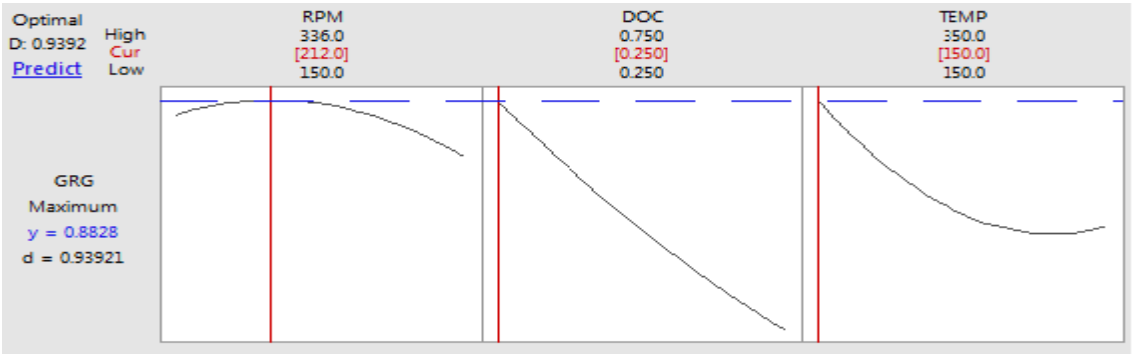

Fig.7: Optimization results of Ra and MRR

3.3 Confirmation test GRG

Confirmatory experiments were carried out to validate the optimization outcomes. Table 5 shows the results of confirmatory tests performed under ideal conditions. The table shows that the error in percentage between projected and experimental outcomes is quite modest, less than 2%. This suggests that the optimized hot turning process factors can be used to get a higher GRG of AISI202 stainless steel.

Table 5. Optimized results for GRG

Optimized condition Response		
A(rpm), GRG	B(mm),	C (^{0}C)
212	0.25	350
Avg. Actual	0.895	
Predicted	0.883	
Error%	1.35	

4. Conclusions

In the current study, we investigated the hot-turning process of AISI 202 at three different workpiece temperatures using an uncoated cutting tool. Our focus was on examining the impact of various turning parameters, including workpiece temperature, depth of cut, cutting speed on-chip geometry, surface roughness, and MRR in comparison to room temperature conditions. The following conclusions can be derived from our findings:

- An increase in workpiece temperature led to an expansion of the chip-tool contact length, accompanied by a reduction in chip thickness.
- At room temperature, chip formation exhibited a short helical pattern. However, at higher workpiece temperatures, we observed the generation of continuous chips with a helical nature, and the serrations in the chips decreased as the workpiece temperature increased.
- Among the factors studied, temperature had the most significant effect on the GRG, followed by hot turning speed and depth of cut.
- We achieved an optimal Grey Relational Grade of 0.907 under the following conditions: hot turning speed of 243rpm, depth of cut of 0.250mm, and workpiece temperature of 350°C.
- Our results demonstrated that the predicted outcomes closely aligned with the results of the confirmatory test, with a percentage error below 2%. This demonstrates the efficacy of the optimization strategy used.
- Regarding potential future research scope, the investigation may be carried out concerning other hard materials like AISI-52100, SAE-01, etc. Several types of other machining processes, like grinding, milling may be considered.

References

1) J. Meng, B. Huang, X. Dong, Y. Hu, Y. Zhao, X. Wei, and X. Luan, “Experimental Investigation on Ultrasonic Atomization Assisted Turning of Titanium Alloy,” *Micromachines*, 11(2) 168 (2020). http://dx.doi.org/10.3390/mi11020168.

2) Ashish Kumar Srivastava, Shashi Prakash Dwivedi, Nagendra Kumar Maurya, and M. Maurya, “3D Visualization and Topographical Analysis in Turning of Hybrid MMC By CNC Lathe SPRINT 16TC Made of BATLIBOI,” *Evergreen*, 7(2) 202–208, (2020). http://dx.doi.org/10.5109/4055217.

3) S. Sharma, K. Mausam, and K. Sharma, “Effects of Nanoparticles on the MRR and TWR of graphene-based Composite by Electro discharge Machining,”

Evergreen, 9(4) 1021–1030 (2022). http://dx.doi.org/10.5109/6625715.

4) A. Sharma, H. Chawla, and K. Srinivas, "Prediction of Surface Roughness of Mild Steel finished with Viscoelastic Magnetic Abrasive Medium," *Evergreen*, 10(2) 1061–1067 (2023). http://dx.doi.org/10.5109/6793663.
5) S. M. Ebrahimi, M. Hadad, A. Araee, and S. H. Ebrahimi, "Influence of machining conditions on tool wear and surface characteristics in hot turning of AISI630 steel," *The International Journal of Advanced Manufacturing Technology*, 114(11–12), 3515–3535 (2021). http://dx.doi.org/10.1007/s00170-021-07106-2.
6) A. K. Parida and K. Maity, "FEM analysis and experimental investigation of force and chip formation on hot turning of Inconel 625," *Defence Technology*, 15(6) 853–860 (2019). http://dx.doi.org/10.1016/j.dt.2019.04.012.
7) A. K. Parida and K. Maity, "Comparison the machinability of Inconel 718, Inconel 625 and Monel 400 in hot turning operation," *Engineering Science and Technology, an International Journal*, 21(3) 364–370 (2018). http://dx.doi.org/10.1016/j.jestch.2018.03.018.
8) K. P. Maity and P. K. Swain, "An experimental investigation of hot-machining to predict tool life," *Journal of Materials Processing Technology*, 198(1–3) 344–349, (2008). http://dx.doi.org/10.1016/j.jmatprotec.2007.07.018.
9) A. Parida and K. Maity, "Heat assisted machining of nickel base alloys: experimental and numerical analysis", PhD diss., 2017.
10) A. K. Parida and K. P. Maity, "An Experimental Investigation to Optimize Multi-Response Characteristics of Ni-Hard Material Using Hot Machining," *Advanced Engineering Forum*, 16 16–23 (2016). http://dx.doi.org/10.4028/www.scientific.net/aef.16.16.
11) L. N. López de lacalle, J. Pérez, J. I. Llorente, and J. A. Sánchez, "Advanced cutting conditions for the milling of aeronautical alloys," *Journal of Materials Processing Technology*, 100(1–3) 1–11 (2000). http://dx.doi.org/10.1016/s0924-0136(99)00372-6.
12) L. N. Lo´pez de Lacalle, J. A. Sa´nchez, A. Lamikiz, and A. Celaya, "Plasma Assisted Milling of Heat-Resistant Superalloys," *Journal of Manufacturing Science and Engineering*, 126(2) 274–285 (2004). http://dx.doi.org/10.1115/1.1644548.
13) A. K. Parida and K. P. Maity, "Optimization in Hot Turning of Nickel Based Alloy Using Desirability Function Analysis," *International Journal of Engineering Research in Africa*, 24 64–70 (2016). http://dx.doi.org/10.4028/www.scientific.net/jera.24.64.
14) C. E. Leshock, J.-N. Kim, and Y. C. Shin, "Plasma enhanced machining of Inconel 718: modeling of workpiece temperature with plasma heating and experimental results," *International Journal of Machine Tools and Manufacture*, 41(6) 877–897 (2001). http://dx.doi.org/10.1016/s0890-6955(00)00106-1.
15) A. K. Parida and K. Maity, "Experimental investigation on tool life and chip morphology in hot machining of Monel-400," *Engineering Science and Technology, an International Journal*, 21(3) 371–379 (2018). http://dx.doi.org/10.1016/j.jestch.2018.04.003.
16) S. Joshi, A. Tewari, and S. S. Joshi, "Microstructural Characterization of Chip Segmentation Under Different Machining Environments in Orthogonal Machining of Ti6Al4V," *Journal of Engineering Materials and Technology*, 137(1) (2015). http://dx.doi.org/10.1115/1.4028841.
17) Y. Kaynak, T. Lu, and I. S. Jawahir, "Cryogenic Machining-Induced Surface Integrity: A Review and Comparison with Dry, MQL, and Flood-Cooled Machining," *Machining Science and Technology*, 18(2) 149–198 (2014). http://dx.doi.org/10.1080/10910344.2014.897836.
18) A. K. M. N. Amin, S. A. Sulaiman, and M. D. Arif, "Development of Mathematical Model for Chip Serration Frequency in Turning of Stainless Steel 304 Using RSM," *Applied Mechanics and Materials*, 217 2206–2209 (2012). http://dx.doi.org/10.4028/www.scientific.net/amm.217-219.2206.
19) M. Bäker, J. Rösler, and C. Siemers, "The influence of thermal conductivity on segmented chip formation," *Computational Materials Science*, 26 175–182 (2003). http://dx.doi.org/10.1016/s0927-0256(02)00396-8.
20) M. Bäker, "The influence of plastic properties on chip formation," *Computational Materials Science*, 28(3–4) 556–562 (2003). http://dx.doi.org/10.1016/j.commatsci.2003.08.013.
21) Y. Qibiao, L. Zhanqiang, and W. Bing, "Characterization of chip formation during machining 1045 steel," *The International Journal of Advanced Manufacturing Technology*, 63(9–12) 881–886 (2012). http://dx.doi.org/10.1007/s00170-012-3954-1.
22) V. Schulze, J. Osterried, H. Meier, and F. Zanger, "Simulation of Multiple Chip Formation when Broaching SAE 5120 Low Alloy Steel," *Advanced Materials Research*, 223 37–45 (2011). http://dx.doi.org/10.4028/www.scientific.net/amr.223.37.
23) J. Hua and R. Shivpuri, "Prediction of chip morphology and segmentation during the machining of titanium alloys," *Journal of Materials Processing Technology*, 150(1–2) 124–133 (2004). http://dx.doi.org/10.1016/j.jmatprotec.2004.01.028.

24) Y. Gao, G. Wang, and B. Liu, “Chip formation characteristics in the machining of titanium alloys: a review,” *International Journal of Machining and Machinability of Materials*, 18(1/2) 155 (2016). http://dx.doi.org/10.1504/ijmmm.2016.075467.
25) S. Kouadri, K. Necib, S. Atlati, B. Haddag, and M. Nouari, “Quantification of the chip segmentation in metal machining: Application to machining the aeronautical aluminium alloy AA2024-T351 with cemented carbide tools WC-Co,” *International Journal of Machine Tools and Manufacture*, 64 102–113, (2013). http://dx.doi.org/10.1016/j.ijmachtools.2012.08.006.
26) Z. C. Lin and Y. Y. Lin, “Three-dimensional elastic–plastic finite element analysis for orthogonal cutting with discontinuous chip of 6-4 brass,” *Theoretical and Applied Fracture Mechanics*, 35(2) 137–153 (2001). http://dx.doi.org/10.1016/s0167-8442(00)00055-0.
27) J. Barry and G. Byrne, “The Mechanisms of Chip Formation in Machining Hardened Steels,” *Journal of Manufacturing Science and Engineering*, 124(3) 528–535 (2002). http://dx.doi.org/10.1115/1.1455643.
28) T. Braham-Bouchnak, G. Germain, A. Morel, and J. L. Lebrun, “The influence of laser assistance on the machinability of the titanium alloy Ti555-3,” *The International Journal of Advanced Manufacturing Technology*, 68(9–12) 2471–2481 (2013). http://dx.doi.org/10.1007/s00170-013-4855-7.
29) A. K. Parida and K. Maity, “Numerical analysis of chip geometry on hot machining of nickel base alloy,” *Journal of the Brazilian Society of Mechanical Sciences and Engineering*, 40(10) (2018). http://dx.doi.org/10.1007/s40430-018-1418-8.
30) A. K. Parida, “Analysis of Chip Geometry in Hot Machining of Inconel 718 Alloy,” *Iranian Journal of Science and Technology, Transactions of Mechanical Engineering*, 43(S1) 155–164 (2018). http://dx.doi.org/10.1007/s40997-018-0146-0.
31) M. Hanief and M. S. Charoo, “Modeling and optimization of flank wear and surface roughness of Monel-400 during hot turning using artificial intelligence techniques,” *Metallurgical and Materials Engineering*, 26(1) 57–69 (2020). http://dx.doi.org/10.30544/473.
32) J. Airao and C. K. Nirala, “Finite Element Modeling and Experimental Validation of Tool Wear in Hot-Ultrasonic-Assisted Turning of Nimonic 90,” *Journal of Vibration Engineering & Technologies*, (2022). http://dx.doi.org/10.1007/s42417-022-00776-6.
33) C. Hartita, and I. Yani, "Surface Roughness Analysis of Hot Turning AISI 4340 Using The Response Surface Methodology", International Journal of Engineering Advanced Research, 5(2) 48-60 (2023).
34) I. Thamrin, A. S. Mohruni, I. Yani, R. Sipahutar and A. Darmalasari, "Surface roughness modelling of AISI 4340 turning with hot machining method using response surface methodology", In AIP Conference Proceedings, 2689(1) (2023).
35) D. Mukherjee, R. Ranjan, and S. C. Moi, “Multi-Response Optimization of Surface Roughness and MRR in Turning using Taguchi Grey Relational Analysis (TGRA),” *International Research Journal of Multidisciplinary Scope*, 03(02) 01–07 (2022). http://dx.doi.org/10.47857/irjms.2022.v03i02.068.
36) A. Kumar, Arindam Kumar Chanda, and S. Angra, “Optimization of Stiffness Properties of Composite Sandwich using Hybrid Taguchi-GRA-PCA,” *Evergreen*, 8(2) 310–317 (2021). http://dx.doi.org/10.5109/4480708.
37) P. Gupta, B. Singh, and Y. Shrivastava, “Theoretical and Experimental Prediction of Optimal Process Variables for Enhanced Metal Removal Rate During Turning on CNC lathe,” *Evergreen*, 10(2) 1127–1132 (2023). http://dx.doi.org/10.5109/6793673.
38) A. Chandra, A. Yadav, S. Singh, and Pawan Kumar Arora, “Optimisation of Machining Parameters for CNC Milling of Fibre Reinforced Polymers,” *Evergreen*, 10(2) 765–773 (2023). http://dx.doi.org/10.5109/6792826.
39) A. Li and J. Zhao, Hou, G. "Effect of cutting speed on chip formation and wear mechanisms of coated carbide tools when ultra-high-speed face milling titanium alloy Ti-6Al-4V", Advances in Mechanical Engineering, 9(7) (2017).
40) R. Ranjan, A. Saha, and A. Kumar Das, “Comparison of Multi-Criteria Decision Making Methods for Multi Optimization of GTAC Process Parameters,” *Periodica Polytechnica Mechanical Engineering*, 66(2) 166–174 (2022). http://dx.doi.org/10.3311/ppme.19835.
41) R. Ranjan and A. Saha, “A novel hybrid multi-criteria optimization of 3D printing process using grey relational analysis (GRA) coupled with principal component analysis (PCA),” *Engineering Research Express*, 6(1), 015080 (2024). http://dx.doi.org/10.1088/2631-8695/ad2320.